Acta Pharmaceutica Sinica B 2023;13(11):4502–4510

Chinese Pharmaceutical Association
Institute of Materia Medica, Chinese Academy of Medical Sciences

Acta Pharmaceutica Sinica B

www.elsevier.com/locate/apsb
www.sciencedirect.com

ORIGINAL ARTICLE

Activation of PXR causes drug interactions with Paxlovid in transgenic mice

Saifei Lei[a], Alice Guo[b], Jie Lu[a], Qian Qi[a], Aaron S. Devanathan[c], Junjie Zhu[a,*], Xiaochao Ma[a,*]

[a]*Center for Pharmacogenetics, Department of Pharmaceutical Sciences, School of Pharmacy, University of Pittsburgh, Pittsburgh, PA 15261, USA*
[b]*School of Nursing, University of Pennsylvania, Philadelphia, PA 19104, USA*
[c]*Department of Pharmacy and Therapeutics, School of Pharmacy, University of Pittsburgh, Pittsburgh, PA 15261, USA*

Received 11 April 2023; received in revised form 11 June 2023; accepted 28 July 2023

KEY WORDS

Paxlovid;
Nirmatrelvir;
Ritonavir;
Pregnane X receptor;
CYP3A4/5;
Rifampicin;
Rhynchophylline;
Drug/herb–drug interactions

Abstract Paxlovid is a nirmatrelvir (NMV) and ritonavir (RTV) co-packaged medication used for the treatment of coronavirus disease 2019 (COVID-19). The active component of Paxlovid is NMV and RTV is a pharmacokinetic booster. Our work aimed to investigate the drug/herb–drug interactions associated with Paxlovid and provide mechanism-based guidance for the clinical use of Paxlovid. By using recombinant human cytochrome P450s (CYPs), we confirmed that CYP3A4 and 3A5 are the major enzymes responsible for NMV metabolism. The role of CYP3A in Paxlovid metabolism were further verified in *Cyp3a*-null mice, which showed that the deficiency of CYP3A significantly suppressed the metabolism of NMV and RTV. Pregnane X receptor (PXR) is a ligand-dependent transcription factor that upregulates CYP3A4/5 expression. We next explored the impact of drug- and herb-mediated PXR activation on Paxlovid metabolism in a transgenic mouse model expressing human PXR and CYP3A4/5. We found that PXR activation increased CYP3A4/5 expression, accelerated NMV metabolism, and reduced the systemic exposure of NMV. In summary, our work demonstrated that PXR activation can cause drug interactions with Paxlovid, suggesting that PXR-activating drugs and herbs should be used cautiously in COVID-19 patients receiving Paxlovid.

*Corresponding authors.
E-mail addresses: juz28@pitt.edu (Junjie Zhu), mxiaocha@pitt.edu (Xiaochao Ma).

Peer review under the responsibility of Chinese Pharmaceutical Association and Institute of Materia Medica, Chinese Academy of Medical Sciences.

https://doi.org/10.1016/j.apsb.2023.08.001

1. Introduction

Coronavirus disease 2019 (COVID-19) is caused by severe acute respiratory syndrome coronavirus 2 (SARS-CoV-2), a highly transmissible and pathogenic virus that significantly threatens public health[1]. Since the outbreak of COVID-19 in 2019, ~757,000,000 confirmed cases including ~6,947,000 deaths have been reported to World Health Organization as of June 2023[2]. In 2022, Paxlovid was approved by the U.S. Food and Drug Administration for COVID-19 treatment. Adults and children who tested positive for SARS-CoV-2 and diagnosed with mild-to-moderate COVID-19 were recommended to take Paxlovid[3]. Paxlovid significantly decreased the risk of progression to severe COVID-19[4]. In addition, Paxlovid remarkably reduced the hospitalization rate and the risk of death from COVID-19[5,6].

Paxlovid is a medication co-packaged with nirmatrelvir (NMV) and ritonavir (RTV). NMV is the active component in Paxlovid, which strongly inhibits SARS-CoV-2 main protease and suppresses virus replication[7]. NMV cannot be used alone because it is rapidly metabolized by cytochrome P450 3A4 (CYP3A4), leading to the loss of efficacy[8]. RTV is a CYP3A4 inhibitor[9], which slows down NMV metabolism and therefore boosts the efficacy of NMV. However, RTV itself is also a CYP3A4 substrate[10], and CYP3A4 inducers accelerates RTV metabolism[11]. Many clinically used drugs are CYP3A4 inducers[12], such as rifampicin (RIF)[13], a first-line drug for the treatment of tuberculosis. In addition, some herbal supplements can also upregulate CYP3A4 expression[14,15]. As reported in the Paxlovid fact sheet, CYP3A4 inducer carbamazepine caused ~50% reduction for NMV exposure, whereas CYP3A4 inhibitor itraconazole increased NMV exposure in healthy subjects[16]. These data raised concerns for the potential drug/herb−drug interactions with Paxlovid through CYP3A4[17].

Pregnane X receptor (PXR) is a key regulator of CYP3A4[13]. Many drugs, including RIF, upregulates CYP3A4 expression through a PXR-dependent pathway[18]. In addition, PXR activators have been identified in CYP3A4-inducing herbs, such as hyperforin from St. John's wort and rhynchophylline (RCP) from Cat's claw[19,20]. Based upon these data, we hypothesized that ligand-dependent activation of PXR causes drug/herb−drug interactions with Paxlovid through CYP3A4 induction. To test this hypothesis, we used RIF and RCP as PXR activators together with PXR-humanized (hPXR) mouse models. The results from our work can be used to guide the clinical use of Paxlovid by targeting PXR.

2. Materials and methods

2.1. Chemical and reagents

NMV was purchased from AmBeed, Inc. (Arlington Heights, IL, USA). RTV and RCP were purchased from Sigma−Aldrich (St. Louis, MO, USA). RIF were purchased from TCI America, Inc. (Portland, OR, USA). Reduced nicotinamide adenine dinucleotide phosphate (NADPH) was purchased from Cayman Chemical Company (Ann Arbor, MI, USA). The recombinant human CYPs and human liver microsomes (HLM) were purchased from Sekisui XenoTech, LLC (Kansas City, KS, USA).

2.2. Animals

To determine the role of CYP3A in the metabolism and pharmacokinetics (PK) of NMV and RTV, we used a hPXR mouse model deficient in *Cyp3a* (hPXR/*Cyp3a*-null). In addition, we used a hPXR mouse model transgenic with human CYP3A4/5/7 (hPXR/CYP3A) and a *Pxr*-null mouse model transgenic with human CYP3A4/5/7 (*Pxr*-null/CYP3A). These mouse models have been described in previous reports[11,21,22]. Briefly, hPXR/*Cyp3a*-null mice express human PXR gene but lack mouse *Pxr* and *Cyp3a* genes. The hPXR/CYP3A mice express human PXR and CYP3A4/5/7 genes but lack mouse *Pxr* and *Cyp3a* genes. The *Pxr*-null/CYP3A mice express human CYP3A4/5/7 genes but lack human PXR and mouse *Pxr* genes. The current work used mice among 6−8 weeks old. This selection is based upon the followings: (1) CYP3As have ontogenic expression patterns showing significant difference between adults and children[23−25]; (2) Paxlovid is authorized for use in adolescents and teenagers ages 12 and up[16]; and our selection of mouse age mimicked the use of Paxlovid in humans as the average age entering puberty is ~42 days (6 weeks) for mice and 11.5 years for humans[26]. To save resources, we only used male mice because PXR can be activated regardless of gender[27−29]. All studies using mice were conducted following the animal protocols approved by the University of Pittsburgh Animal Care and Use Committee.

2.3. Metabolism of NMV in HLM

Incubations were carried out in 1 × PBS (pH 7.4), containing 0.1 mg HLM, 20 μmol/L NMV, with or without 1 mmol/L NADPH in a final volume of 100 μL. The reactions were allowed to continue at 37 °C for 1 h. Afterward, the reactions were terminated by adding 100 μL of methanol/acetonitrile (1:1, *v*/*v*) to precipitate proteins. The NMV metabolites were analyzed by the ultra-high performance liquid chromatography coupled with quadrupole time-of-flight mass spectrometry (UPLC−Q-TOF-MS, Waters Corporation, Milford, MA, USA).

2.4. UPLC−Q-TOF-MS analysis

Drug metabolites were separated by an Acquity UPLC BEH C18 column (Waters Corporation, Milford, MA, USA). The column temperature was set at 50 °C. The mobile phases included 0.1% formic acid in water (A) and 0.1% formic acid in acetonitrile (B). The elution gradient was set as follows: 0.0−1.0 min, 2% B; 1.0−8 min, 2%−95% B; 8−12.5 min, 95% B; 12.5−13 min, 95%−2% B; 13−15 min, 2% B. The flow rate was set at 0.5 mL/min. The Q-TOF-MS system was operated in both positive and negative mode with electrospray ionization. Collision energy ramping from 10 to 30 eV was used for structural elucidation of drug metabolites. Q-TOF-MS was calibrated with sodium formate and monitored by the intermittent injection of leucine enkephalin as lock mass in real time. For the quantification of NMV and RTV, the calibration range was 1−1000 ng/mL, and the accuracy was within the range of ±15% from the intra- and inter-day tests.

2.5. Metabolomic profiling of NMV metabolites

The data from UPLC−Q-TOF-MS analysis were acquired by MassLynx 4.1 and then transformed to Markerlynx XS (Waters Corporation, Milford, MA, USA). Next, the data matrix was exported into SIMCA-P (Version 13, Umetrics, Kinnelon, NJ, USA) for orthogonal partial least-squares discriminant analysis (OPLS-DA). S-plot and trend-plot were generated and used for screening of NMV metabolites. The structures of NMV

metabolites were predicted based on accurate mass measurement and tandem mass spectrometry (MS/MS) fragmentation.

2.6. *Metabolism of NMV by recombinant CYPs*

Recombinant CYPs were used to determine the role of individual CYP in NMV metabolism. In brief, incubations were performed in 1 × PBS, containing 20 μmol/L NMV, 10 pmol of each CYP (control, CYP1A2, 2A6, 2B6, 2C8, 2C9, 2C19, 2D6, 2E1, 3A4, and 3A5), and 1 mmol/L NADPH in a final volume of 100 μL. After incubating at 37 °C for 1 h, reactions were terminated by adding 100 μL of methanol/acetonitrile (1:1, *v*/*v*). NMV metabolites were extracted and analyzed by UPLC−Q-TOF-MS.

2.7. *Metabolism of NMV in liver S9 from mice pretreated with PXR activators*

hPXR/CYP3A and *Pxr*-null/CYP3A mice were pretreated with RIF (50 mg/kg RIF in diet) for 7 days or RCP (60 mg/kg, *po*, bid) for 4 days. Liver S9 was prepared and used to determine the impact of PXR activation on NMV metabolism. Briefly, the incubation was conducted in 1 × PBS, containing 20 μmol/L NMV, 1 mg/mL liver S9, and 1 mmol/L NADPH in a final volume of 100 μL. After 1 h incubation at 37 °C, NMV metabolites were analyzed by UPLC−Q-TOF-MS.

2.8. *PK of Paxlovid*

To determine the impact of CYP3A deficiency on the PK of Paxlovid, hPXR/*Cyp3a*-null and hPXR/CYP3A mice were treated orally with the mixture of RTV (20 mg/kg) and NMV (60 mg/kg). To determine the impact of PXR activation on the PK of Paxlovid, hPXR/CYP3A mice were pretreated with control, RIF (50 mg/kg RIF in diet, 7 days) or RCP (60 mg/kg, *po*, bid, 4 days), followed by the treatment with the mixture of RTV (20 mg/kg) and NMV (60 mg/kg). RIF is an anti-tuberculosis drug and the dose of RIF is < 10 mg/kg for adults[30]. The converted dose of RIF from humans to mice is < 120 mg/kg. In the current work, RIF was mixed in diet (50 mg RIF in 1 kg diet), which resulted in a dose of RIF at 10−20 mg/kg in mice. This approach has been verified for PXR activation in our previous reports[11,31]. As for RCP, it is a major and active component in herbs Cat's claw and Gou Teng[19]. Because of the lack of guidance and regulations for the clinical use of herbal medicines or supplements, their doses vary a lot among populations. We used RCP at 60 mg/kg for mouse studies, which equals ∼5 mg/kg in humans. Blood was collected from 0 to 8 h after Paxlovid treatment. Serum was prepared and used for analysis of NMV and RTV by UPLC−Q-TOF-MS. PK parameters of RTV and NMV were calculated by Phoenix WinNonlin using noncompartmental analysis (Certara, Inc., Cary, NC, USA).

2.9. *Expression of CYP3A*

A real-time polymerase chain reaction (qPCR) and Western blotting were conducted to analyze CYP3A expression. Briefly, RNA was extracted from liver tissues using TRIzol reagent (Invitrogen, Carlsbad, CA, USA). Next, RNA was reverse transcribed into cDNA using M-MLV reverse transcriptase (Invitrogen, Waltham, MA, USA). qPCR was performed using SYBR Green PCR Master Mix (Applied Biosystems, Waltham, MA, USA). The primers used for *CYP3A4* and *CYP3A5* mRNA analysis are listed in Supporting Information Table S1. For Western blotting, the total proteins in liver homogenates were used to determine CYP3A protein expression. In brief, liver proteins were separated through SDS-polyacrylamide gel electrophoresis followed by protein transfer to PVDF membranes. Proteins were then probed using primary antibodies against CYP3A (Fitzgerald, Acton, MA, USA) and detected by a chemiluminescence method. *Cyclophilin* and glyceraldehyde-3-phosphate dehydrogenase (*GAPDH*) were used as an internal control for qPCR and Western blotting, respectively.

2.10. *Data analysis*

Data are presented as mean ± standard deviation (SD). Student's *t*-test was performed using GraphPad Prism to determine the differences between two groups. $P < 0.05$ was accepted as statistical significance.

3. Results

3.1. *Identification of NMV metabolites*

A metabolomic approach was used to identify NMV metabolites in the incubation with HLM. Three incubation groups of NMV were well-separated into the corresponding clusters by OPLS-DA analysis (Fig. 1A). NMV metabolites (M1−M7) ranked high in the S-plot (Fig. 1B), and they were only detected in the incubation group with NMV, HLM, and NADPH (Fig. 1C). By analyzing the exact mass, MS/MS fragmentation, and retention time[8], M1−M4 were determined as mono-hydroxylation products of NMV (Fig. 1D and E, Supporting Information Table S2 and Fig. S1). M5 has a protonated molecular ion [M+H] at *m/z* = 498.2324 indicating that M5 is a dehydrogenated metabolite of NMV (Supporting Information Table S2, Fig. S2A and S2B). NMV metabolites M1−M5 are consistent with a previous report[8].

M6 and M7 are newly identified NMV metabolites. M6 was eluted at 4.37 min and has a deprotonated molecular ion [M−H] at *m/z* = 530.2239, suggesting an addition of two oxygen atoms to NMV (Table S2, Fig. S2C and S2D). The fragmental ions at *m/z* = 378 and 224 suggest oxidations at the pyrrolidone and *t*-butyl moiety of M6, respectively (Fig. S2D). M7 has a deprotonated molecular ion [M−H] at *m/z* = 512.2117, indicating a loss of two protons and an addition of oxygen atom (Table S2, and Fig. S2E and S2F). The fragmental ion at *m/z* = 362 suggests the intact of whole *t*-butyl moiety and the oxidation at the pyrrolidone moiety (Fig. S2F). Overall, our study identified 7 NMV metabolites in the incubation with HLM.

3.2. *Roles of CYPs in NMV metabolism*

Recombinant human CYPs including 1A2, 2A6, 2B6, 2C8, 2C9, 2C19, 2D6, 2E1, 3A4, and 3A5 were used to determine which specific CYP contributes to NMV metabolism. CYP3A4 was determined as the key enzyme in NMV metabolism, which contributed the most to all the 7 metabolic pathways of NMV (Fig. 2A−D, Supporting Information Fig. S3). Notably, CYP3A5 was also involved in the 7 metabolic pathways of NMV, especially for the production of M4 and M5 (Fig. 2A−D and Fig. S3). In addition, CYP2C8 could also catalyze NMV to produce a small

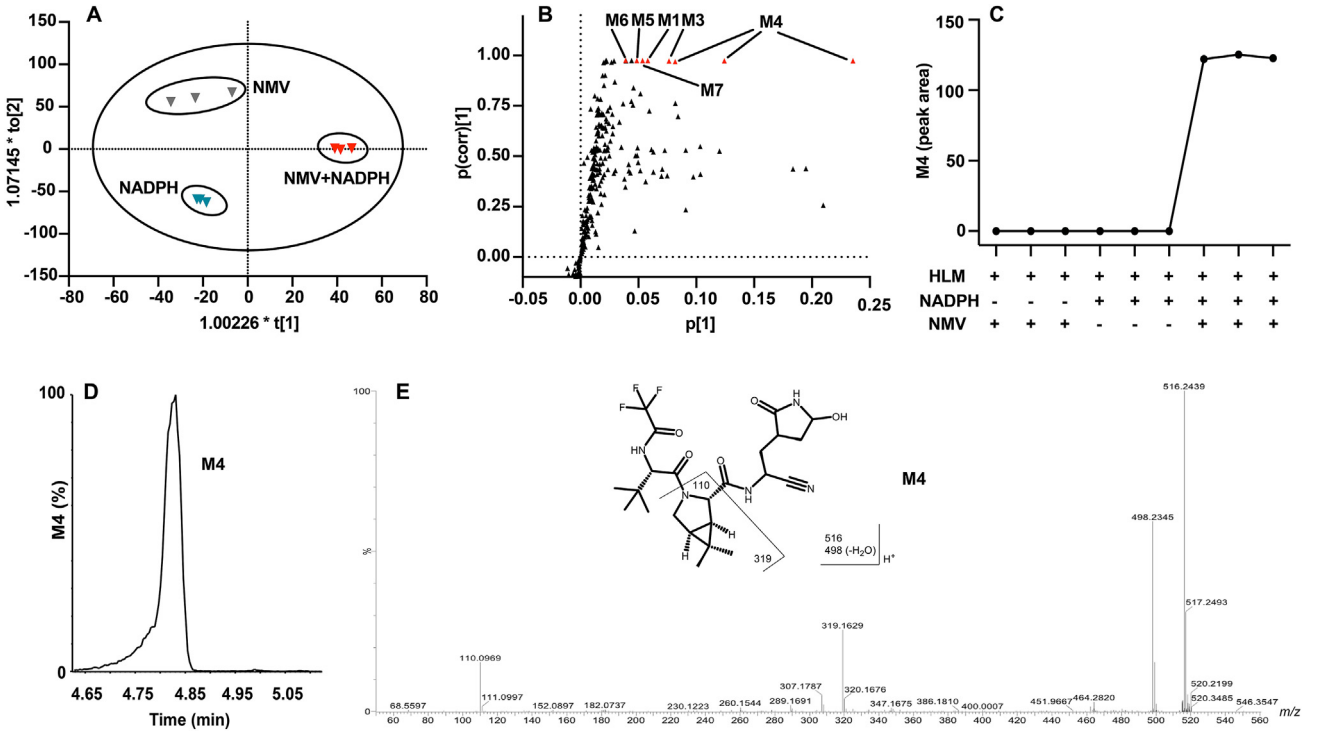

Figure 1 Metabolomic profiling of NMV metabolism in human liver microsomes (HLM). (A) A score plot showing the differentiation of the three incubation groups of NMV with or without NADPH. (B) A loading S-plot highlighting ions that were NMV metabolites. (C) A trend plot showing that M4 was only produced in the incubation group with NMV, HLM, and NADPH. The *Y* axis is the relative abundance of M4, quantified in peak areas. (D) The chromatogram of M4. The *Y* axis is the percentage of M4 when normalized to the maximum response in the window. (E) The MS/MS spectrum and chemical structure of M4. The *X* axis is mass to charge ratio (*m/z*) and the *Y* axis is the percentage of MS fragments when normalized to the maximum response in the window.

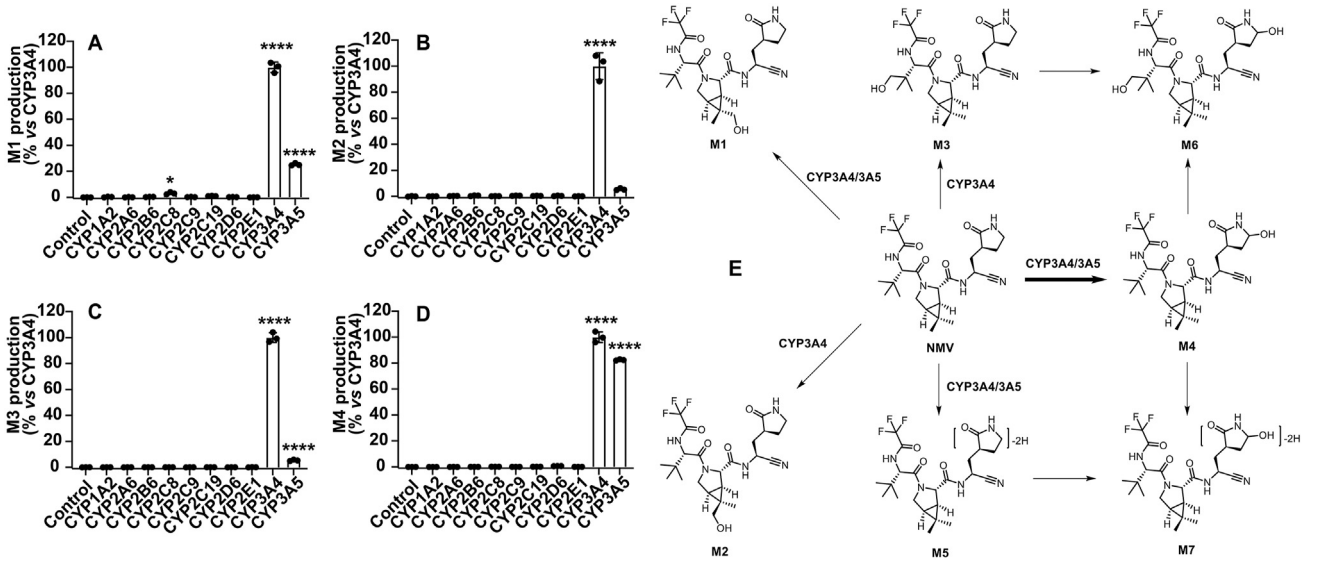

Figure 2 Roles of CYPs in NMV metabolism. (A−D) The formation of NMV metabolites M1 (A), M2 (B), M3 (C), and M4 (D) in the incubation with recombinant CYPs. NMV metabolites were detected by UPLC−Q-TOF-MS. The data in CYP3A4 group are set as 100% and expressed as mean ± SD ($n = 3$); ****$P < 0.0001$ *vs.* control. (E) A metabolic map of NMV.

amount of M1 (Fig. 2A). Other CYPs including CYP1A2, 2A6, 2B6, 2C9, 2C19, 2D6, and 2E1 did not contribute to NMV metabolism (Fig. 2A−D and Fig. S3). Overall, CYP3A4 and 3A5 are the predominant enzymes responsible for NMV metabolism (Fig. 2E).

3.3. *Impact of CYP3A deficiency on the PK of Paxlovid*

To further validate the role of CYP3A in Paxlovid metabolism, PK studies of Paxlovid were conducted using hPXR/CYP3A and

hPXR/*Cyp3a*-null mice. As expected, the metabolism of both RTV and NMV was significantly suppressed in hPXR/*Cyp3a*-null mice (Fig. 3). The serum concentration−time curve of RTV was remarkably higher in hPXR/*Cyp3a*-null mice than that in hPXR/CYP3A mice (Fig. 3A). Additionally, the area under the curve (AUC) and the maximum concentrations (C_{max}) of RTV in serum were increased by 12.2- and 18.8-fold, respectively, in hPXR/*Cyp3a*-null mice when compared to hPXR/CYP3A mice (Fig. 3B and C). Similar to RTV, the AUC and C_{max} of NMV in serum were also significantly increased in hPXR/*Cyp3a*-null mice when compared to hPXR/CYP3A mice (Fig. 3D−F). These data confirmed that CYP3A is essential for Paxlovid metabolism.

3.4. *PXR activation accelerates NMV metabolism*

In the liver of hPXR/CYP3A mice pretreated with RIF, a well-known human PXR activator[13,32], the mRNA expression levels of CYP3A4 and 3A5 were significantly increased (Fig. 4A and B). High levels of CYP3A protein were also observed in the liver of hPXR/CYP3A mice pretreated with RIF (Fig. 4C). Consistent with the RIF-mediated upregulation of CYP3A, the production of NMV metabolites was remarkably increased in the incubation with the liver S9 fraction of hPXR/CYP3A mice pretreated with RIF (Fig. 4D−G and Supporting Information Fig. S4). Similar results were noted from the studies of RCP, a PXR activator identified from herbs Cat's claw and Gou Teng[19], as the mRNA expression of CYP3A4 and 3A5 was significantly upregulated by RCP in the liver of hPXR/CYP3A mice (Fig. 5A and B). Treatment with RCP also increased the protein level of CYP3A in the liver of hPXR/CYP3A mice, but not in *Pxr*-null/CYP3A mice (Fig. 5C), indicating that RCP-mediated CYP3A upregulation is PXR-dependent. In addition, the production of NMV metabolites was significantly increased in the incubation with the liver S9 fraction of hPXR/CYP3A mice pretreated with RCP (Fig. 5D−G and Supporting Information Fig. S5). These data demonstrated that ligand-dependent activation of PXR induces CYP3A4 and 3A5 expression and accelerates NMV metabolism.

3.5. *Effects of PXR activators on the PK of Paxlovid*

Next, we investigated the effects of PXR activators on the PK of Paxlovid using hPXR/CYP3A mice. In these mice pretreated with RIF, the serum concentration−time curve of NMV was remarkably lower than the control group (Fig. 6A). Additionally, the AUC and C_{max} of NMV in the serum of hPXR/CYP3A mice pretreated with RIF decreased by 82.3% and 59.9%, respectively, when compared to the control group (Fig. 6B and C). Similar results were observed in hPXR/CYP3A mice pretreated with RCP, as the AUC and C_{max} of NMV in serum were also significantly decreased when compared to the control group (Fig. 6D−F). As for RTV, its AUC and C_{max} were also decreased in hPXR/CYP3A mice pretreated with RIF or RCP (Supporting Information Fig. S6). These data indicate that lead-in treatment with PXR activators accelerates CYP3A-mediated Paxlovid metabolism, resulting in low levels of NMV in serum (Fig. 6G).

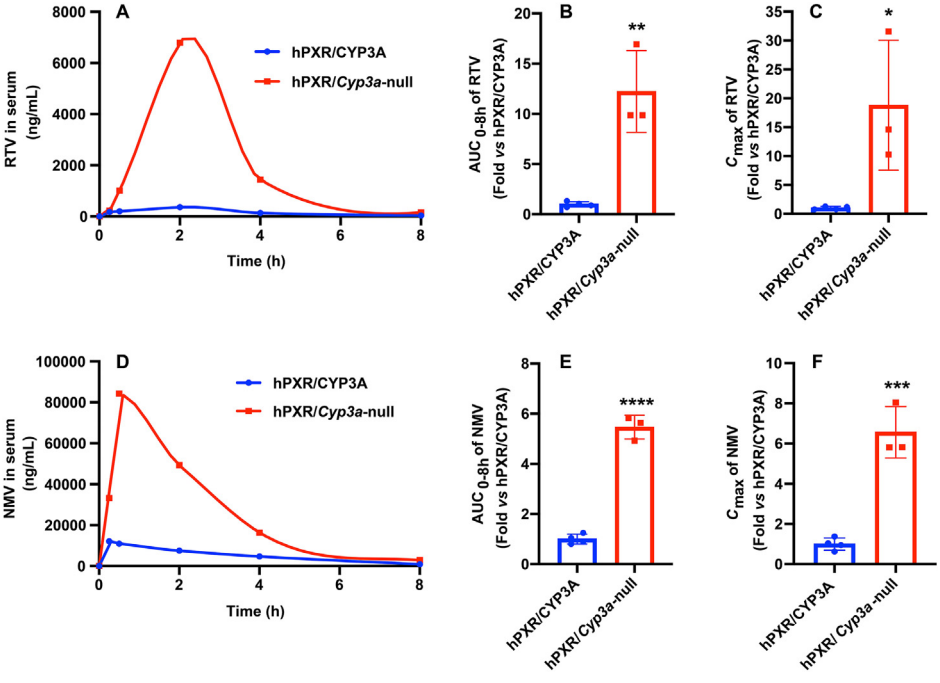

Figure 3 Impact of CYP3A deficiency on the pharmacokinetics (PK) of Paxlovid (NMV/r). hPXR/CYP3A and hPXR/*Cyp3a*-null mice were treated orally with NMV and RTV. Blood samples were collected from 0 to 8 h after NMV/r treatment ($n = 3$ or 4 at each time point). (A, D) Impact of CYP3A deficiency on the concentration−time curve of RTV (A) and NMV (D) in serum. Data are expressed as mean. (B, E) The area under the curve (AUC) of RTV (B) and NMV (E) in serum. (C, F) The maximum concentrations (C_{max}) of RTV (C) and NMV (F) in serum. Data are expressed as mean ± SD. $^*P < 0.05$, $^{**}P < 0.01$, $^{***}P < 0.001$, and $^{****}P < 0.0001$ *vs.* hPXR/CYP3A group.

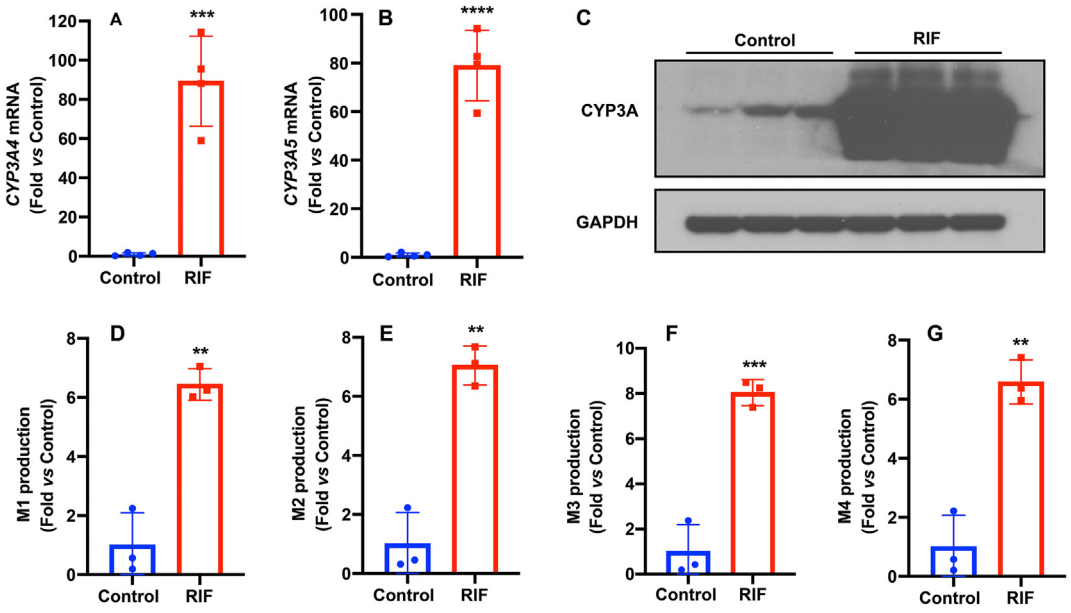

Figure 4 RIF-mediated PXR activation induces CYP3A4/5 expression and accelerates NMV metabolism. hPXR/CYP3A mice were treated with RIF for 1 week. (A, B) The mRNA expression of CYP3A4 (A) and 3A5 (B) in the liver of hPXR/CYP3A mice after RIF treatment. (C) The protein expression of CYP3A in the liver of hPXR/CYP3A mice after RIF treatment. (D−G) Pretreatment with RIF increased the production of NMV metabolites M1 (D), M2 (E), M3 (F), and M4 (G). NMV was incubated in the liver S9 of hPXR/CYP3A mice pretreated with RIF. NMV metabolites were detected by UPLC−Q-TOF-MS. Data are expressed as mean ± SD ($n = 3$); $^{**}P < 0.01$, $^{***}P < 0.001$, and $^{****}P < 0.0001$ *vs.* control.

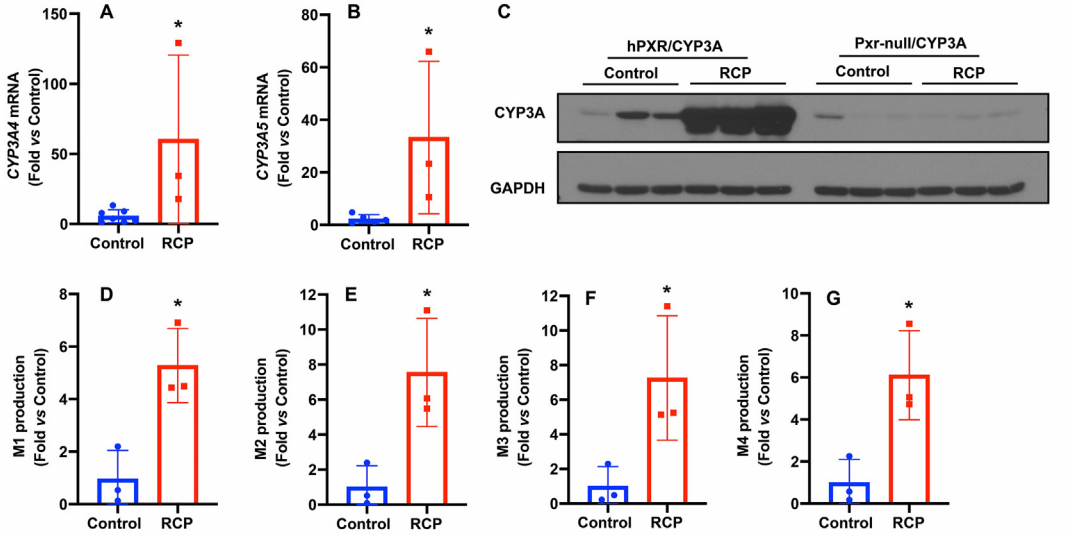

Figure 5 RCP-mediated PXR activation induces CYP3A4/5 expression and accelerates NMV metabolism. hPXR/CYP3A and *Pxr*-null/CYP3A mice were treated with RCP for 4 days. (A, B) The mRNA expression of CYP3A4 (A) and 3A5 (B) in the liver of hPXR/CYP3A mice after RCP treatment. (C) The protein expression of CYP3A in the liver of hPXR/CYP3A and *Pxr*-null/CYP3A mice after RCP treatment. (D−G) Pretreatment with RCP increased the production of NMV metabolites M1 (D), M2 (E), M3 (F), and M4 (G). NMV was incubated in the liver S9 of hPXR/CYP3A mice pretreated with RCP. NMV metabolites were detected by UPLC−Q-TOF-MS. Data are expressed as mean ± SD ($n = 3$); $^{*}P < 0.05$ *vs.* control.

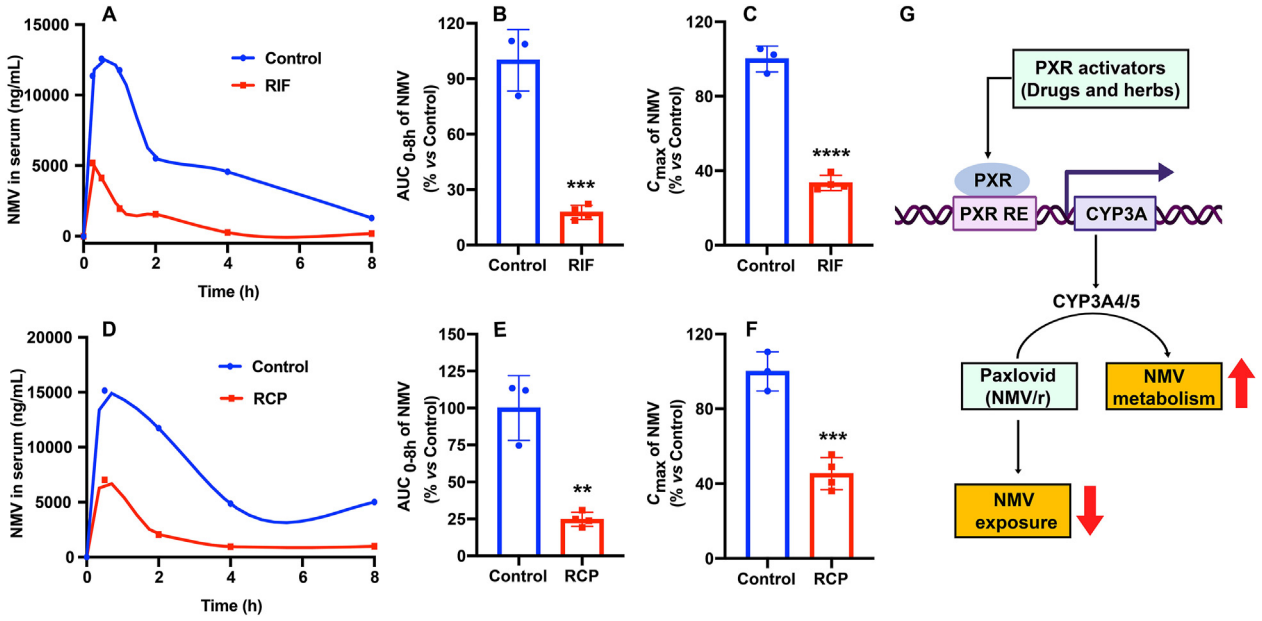

Figure 6 Effects of PXR activators on the PK of NMV in hPXR/CYP3A mice receiving Paxlovid (NMV/r). hPXR/CYP3A mice were pretreated with PXR activators RIF or RCP followed by NMV/r. Blood samples were collected from 0 to 8 h after NMV/r treatment ($n = 3$ or 4 at each time point). (A, D) Effects of RIF (A) and RCP (D) on the concentration−time curve of NMV. Data are expressed as mean. (B, E) Effects of RIF (B) and RCP (E) on the AUC of NMV in serum. (C, F) Effects of RIF (C) and RCP (F) on the C_{max} of NMV in serum. Data are expressed as mean ± SD; $^{**}P < 0.01$ and $^{***}P < 0.001$ *vs.* control group. (G) A diagram showing the role of PXR and CYP3A in drug- and herb-interactions with Paxlovid. Drug- or herb-mediated PXR activation upregulates CYP3A4 and 3A5 expression, which in turn accelerates NMV metabolism and reduces the systemic exposure of NMV. PXR RE, PXR response element. The diagram was created with BioRender.

4. Discussion

Potential drug−drug interactions have been forecasted for COVID-19 patients receiving Paxlovid, especially for the patients with polypharmacy[9,33−35]. To address this concern, researchers have applied physiologically-based PK modeling to predict drug−Paxlovid interactions[36]. However, all these potential interactions have not been verified in bench-based research. In the current work, we conducted a series of studies by profiling NMV metabolic pathways and investigating the effects of PXR-mediated CYP3A induction on NMV metabolism and PK. We demonstrated that PXR is a key modulator for drug/herb−Paxlovid interactions.

PXR is a xenobiotic sensor that can be activated by many commonly used drugs[37]. According to a report from the National Institutes of Health Chemical Genomics Center Pharmaceutical Collection, about 200 clinically used drugs can activate PXR and 106 of them have an $EC_{50} < 10$ μmol/L for PXR activation[18]. Activation of PXR upregulates the expression of drug metabolizing enzymes, such as CYP3A4, and in turn increases the metabolism and elimination of xenobiotics[38]. Our previous work revealed that RIF-mediated PXR activation increased the metabolism of RTV[11]. In the current work, we found that RIF-mediated PXR activation accelerated the metabolism of NMV and decreased its systemic exposure. These results suggest that lead-in or cotreatment with drugs as PXR activators can cause drug−Paxlovid interactions, and potentially decrease its efficacy against SARS-CoV-2.

In addition to clinically used drugs, many herbal supplements can activate PXR, such as St. John's wort, Cat's claw, and *Glycyrrhiza glabra*[19,20,39]. Because of the popularity of herbal supplements in daily life[40], COVID-19 patients may encounter with PXR-activating herbs during Paxlovid therapy. Indeed, some herbal supplements have been used or considered for the treatment of COVID-19[41]. Studies have shown the beneficial effects of *Glycyrrhiza glabra* in attenuating the symptoms of COVID-19[42,43]. Cat's claw also showed its potential for the treatment of COVID-19 because it has anti-SARS-CoV-2 activity[44,45]. However, there is no mechanism-based guidance for the co-treatment of herbal supplements with Paxlovid. By using RCP, an extract from Cat's claw that activates PXR[19], we showed that RCP-mediated PXR activation induced CYP3A expression and increased NMV metabolism and elimination. Our data sound the alarm for the risk of herb−Paxlovid interactions through PXR.

In clinical studies, co-administration of carbamazepine, a CYP3A inducer, resulted in ∼50% decrease in AUC and C_{max} of NMV[16]. However, no data are currently available regarding the interaction of RIF and NMV. Our work showed that pretreatment with RIF led to ∼80% decrease in AUC and 60% decrease in C_{max} of NMV in hPXR/CYP3A mice receiving Paxlovid. Our data are consistent with the carbamazepine data because RIF is a much stronger CYP3A inducer when compared to carbamazepine[46−48]. Clinical studies of Paxlovid also showed that Itraconazole, a CYP3A inhibitor, increased the systemic exposure of NMV[16]. Our current work did not use CYP3A inhibitors but used *Cyp3a*-null mice. We found that genetic deficiency of CYP3A dramatically suppressed NMV metabolism. The results from these two independent studies are consistent because: (1) the dose of Itraconazole in the clinical studies is low and its concentration is dynamically decreasing after treatment, leading to a low level of inhibition on CYP3A; and (2) CYP3As are fully knocked out in the *Cyp3a*-null mice and all CYP3A-mediated metabolic

pathways are shut down. These data are also supported by our enzymatic results showing that all the metabolic pathways of NMV are CYP3A-dependent (Fig. 2).

PXR activation has also been determined as a risk factor for the drug-induced liver injury caused by RTV-containing regimens[11]. In multiple clinical trials, liver damage was observed in 100% of subjects who were pretreated with RIF or efavirenz followed an RTV-containing regimen, such as atazanavir plus RTV, lopinavir plus RTV, and saquinavir plus RTV[49−52]. Both RIF and efavirenz are potent human PXR activators[53−55]. In a follow-up study using genetically engineered PXR mouse models, PXR was determined as a key mediator in the above-mentioned adverse drug interactions, and CYP3A-mediated RTV bioactivation was proposed as the cause of toxicity[11]. Paxlovid is also an RTV-containing regimen. Therefore, we suggest that liver functions should be monitored in COVID-19 patients who are under Paxlovid treatment and have a recent medication history with PXR-activating drugs or herbs.

5. Conclusions

The current work started with the metabolic profiling of NMV, the active component in Paxlovid. We identified 7 NMV metabolites and determined CYP3A4 and 3A5 as the key enzymes responsible for NMV metabolism. The role of CYP3A in Paxlovid metabolism was further verified using *Cyp3a*-null mice, which showed that the deficiency of CYP3A suppressed the metabolism and elimination of NMV and RTV. Using the transgenic mouse models expressing human PXR and CYP3A, our studies revealed that RIF- and RCP-mediated PXR activation induced CYP3A expression and accelerated NMV metabolism, leading to the low systemic exposure of NMV. These data suggest that PXR activators can cause drug interactions with Paxlovid, and potentially decrease its efficacy for COVID-19 therapy.

Acknowledgments

This study was supported in part by the National Center for Complementary and Integrative Health (R21AT011088, USA), the National Institute of Diabetes and Digestive and Kidney Diseases (R01DK126875, USA), and the National Institute of Allergy and Infectious Diseases (R01AI131983, USA). Phoenix WinNonlin was generously provided to the University of Pittsburgh School of Pharmacy by Certara, Inc., through the Center of Excellence Program for academic institutions.

Author contributions

Saifei Lei: Conceptualization, Methodology, Formal analysis, Investigation, Writing-original draft, Writing-review and editing. Alice Guo: Investigation, Writing-review and editing. Jie Lu: Investigation. Qian Qi: Investigation, Writing-review and editing. Aaron S. Devanathan: Resource, Investigation, Writing-review and editing. Junjie Zhu: Methodology, Formal analysis, Investigation, Writing-original draft, Writing-review and editing. Xiaochao Ma: Conceptualization, Writing-review and editing, Supervision, Funding acquisition.

Conflicts of interest

The authors declare no conflicts of interest.

Appendix A. Supporting information

Supporting data to this article can be found online at https://doi.org/10.1016/j.apsb.2023.08.001.

References

1. Tsai PH, Lai WY, Lin YY, Luo YH, Lin YT, Chen HK, et al. Clinical manifestation and disease progression in COVID-19 infection. *J Chin Med Assoc* 2021;**84**:3−8.
2. Organization WH. WHO coronavirus (COVID-19), overview. Updated [2023/06/20]. Accessed [2023/06/29]. Available from: https://covid19.who.int/.
3. Pfizer. Paxlovid. Accessed [2023/06/29]. Available from: https://www.paxlovid.com/.
4. Hammond J, Leister-Tebbe H, Gardner A, Abreu P, Bao W, Wisemandle W, et al. Oral Nirmatrelvir for high-risk, nonhospitalized adults with Covid-19. *N Engl J Med* 2022;**386**:1397−408.
5. Arbel R, Wolff Sagy Y, Hoshen M, Battat E, Lavie G, Sergienko R, et al. Nirmatrelvir use and severe Covid-19 outcomes during the omicron surge. *N Engl J Med* 2022;**387**:790−8.
6. Wong CKH, Au ICH, Lau KTK, Lau EHY, Cowling BJ, Leung GM. Real-world effectiveness of molnupiravir and nirmatrelvir plus ritonavir against mortality, hospitalisation, and in-hospital outcomes among community-dwelling, ambulatory patients with confirmed SARS-CoV-2 infection during the omicron wave in Hong Kong: an observational study. *Lancet* 2022;**400**:1213−22.
7. Saravolatz LD, Depcinski S, Sharma M. Molnupiravir and nirmatrelvir−ritonavir: oral coronavirus disease 2019 antiviral drugs. *Clin Infect Dis* 2023;**76**:165−71.
8. Eng H, Dantonio AL, Kadar EP, Obach RS, Di L, Lin J, et al. Disposition of nirmatrelvir, an orally bioavailable inhibitor of SARS-CoV-2 3C-like protease, across animals and humans. *Drug Metab Dispos* 2022;**50**:576−90.
9. Marzolini C, Kuritzkes DR, Marra F, Boyle A, Gibbons S, Flexner C, et al. Recommendations for the management of drug−drug interactions between the COVID-19 antiviral nirmatrelvir/ritonavir (Paxlovid) and comedications. *Clin Pharmacol Ther* 2022;**112**:1191−200.
10. Sevrioukova IF, Poulos TL. Structure and mechanism of the complex between cytochrome P4503A4 and ritonavir. *Proc Natl Acad Sci U S A* 2010;**107**:18422−7.
11. Shehu AI, Lu J, Wang P, Zhu J, Wang Y, Yang D, et al. Pregnane X receptor activation potentiates ritonavir hepatotoxicity. *J Clin Invest* 2019;**129**:2898−903.
12. Zhou SF. Drugs behave as substrates, inhibitors and inducers of human cytochrome P450 3A4. *Curr Drug Metabol* 2008;**9**:310−22.
13. Lehmann JM, McKee DD, Watson MA, Willson TM, Moore JT, Kliewer SA. The human orphan nuclear receptor PXR is activated by compounds that regulate *CYP3A4* gene expression and cause drug interactions. *J Clin Invest* 1998;**102**:1016−23.
14. Lau C, Mooiman KD, Maas-Bakker RF, Beijnen JH, Schellens JH, Meijerman I. Effect of Chinese herbs on CYP3A4 activity and expression *in vitro*. *J Ethnopharmacol* 2013;**149**:543−9.
15. Hellum BH, Hu Z, Nilsen OG. The induction of CYP1A2, CYP2D6 and CYP3A4 by six trade herbal products in cultured primary human hepatocytes. *Basic Clin Pharmacol Toxicol* 2007;**100**:23−30.
16. Pfizer. Fact sheet for healthcare providers: emergency use authorization for Paxlovid. Updated [2023/05]. Accessed [2023/06/29]. Available from: https://www.fda.gov/media/155050/download.
17. Ye L, Fan S, Zhao P, Wu C, Liu M, Hu S, et al. Potential herb−drug interactions between anti-COVID-19 drugs and traditional Chinese medicine. *Acta Pharm Sin B* 2023;**13**:3598−637.
18. Shukla SJ, Sakamuru S, Huang R, Moeller TA, Shinn P, Vanleer D, et al. Identification of clinically used drugs that activate pregnane X receptors. *Drug Metab Dispos* 2011;**39**:151−9.

19. Lei S, Lu J, Cheng A, Hussain Z, Tidgewell K, Zhu J, et al. Identification of PXR activators from *Uncaria rhynchophylla* (Gou Teng) and *Uncaria tomentosa* (Cat's Claw). *Drug Metab Dispos* 2023;**51**:629−36.
20. Moore LB, Goodwin B, Jones SA, Wisely GB, Serabjit-Singh CJ, Willson TM, et al. St. John's wort induces hepatic drug metabolism through activation of the pregnane X receptor. *Proc Natl Acad Sci U S A* 2000;**97**:7500−2.
21. Cheng J, Ma X, Gonzalez FJ. Pregnane X receptor- and CYP3A4-humanized mouse models and their applications. *Br J Pharmacol* 2011;**163**:461−8.
22. van Herwaarden AE, Wagenaar E, van der Kruijssen CM, van Waterschoot RA, Smit JW, Song JY, et al. Knockout of cytochrome P450 3A yields new mouse models for understanding xenobiotic metabolism. *J Clin Invest* 2007;**117**:3583−92.
23. de Wildt SN, Kearns GL, Leeder JS, van den Anker JN. Cytochrome P450 3A: ontogeny and drug disposition. *Clin Pharmacokinet* 1999;**37**: 485−505.
24. Yu AM, Fukamachi K, Krausz KW, Cheung C, Gonzalez FJ. Potential role for human cytochrome P450 3A4 in estradiol homeostasis. *Endocrinology* 2005;**146**:2911−9.
25. Li Y, Cui Y, Hart SN, Klaassen CD, Zhong XB. Dynamic patterns of histone methylation are associated with ontogenic expression of the *Cyp3a* genes during mouse liver maturation. *Mol Pharmacol* 2009;**75**:1171−9.
26. Dutta S, Sengupta P. Men and mice: relating their ages. *Life Sci* 2016; **152**:244−8.
27. Chen J, Raymond K. Roles of rifampicin in drug−drug interactions: underlying molecular mechanisms involving the nuclear pregnane X receptor. *Ann Clin Microbiol Antimicrob* 2006;**5**:3.
28. Wenk M, Todesco L, Krahenbuhl S. Effect of St John's wort on the activities of CYP1A2, CYP3A4, CYP2D6, *N*-acetyltransferase 2, and xanthine oxidase in healthy males and females. *Br J Clin Pharmacol* 2004;**57**:495−9.
29. Mannel M. Drug interactions with St John's wort: mechanisms and clinical implications. *Drug Saf* 2004;**27**:773−97.
30. Drugs.com. Rifampin dosage. Accessed [2023/06/29]. Available from: https://www.drugs.com/dosage/rifampin.html.
31. Shehu AI, Zhu J, Li J, Lu J, McMahon D, Xie W, et al. Targeting xenobiotic nuclear receptors PXR and CAR to prevent cobicistat hepatotoxicity. *Toxicol Sci* 2021;**181**:58−67.
32. Li T, Chiang JY. Rifampicin induction of CYP3A4 requires pregnane X receptor cross talk with hepatocyte nuclear factor 4alpha and coactivators, and suppression of small heterodimer partner gene expression. *Drug Metab Dispos* 2006;**34**:756−64.
33. Quah KSE, Huang X, Renia L, Oon HH. Drug interactions between common dermatological medications and the oral anti-COVID-19 agents nirmatrelvir-ritonavir and molnupiravir. *Ann Acad Med Singapore* 2022;**51**:774−86.
34. Ross SB, Bortolussi-Courval E, Hanula R, Lee TC, Goodwin Wilson M, McDonald EG. Drug interactions with nirmatrelvir−ritonavir in older adults using multiple medications. *JAMA Netw Open* 2022;**5**:e2220184.
35. Ross SB, Wilson MG, Papillon-Ferland L, Elsayed S, Wu PE, Battu K, et al. COVID-SAFER: deprescribing guidance for hydroxychloroquine drug interactions in older adults. *J Am Geriatr Soc* 2020;**68**:1636−46.
36. Wang Z, Chan ECY. Physiologically-based pharmacokinetic modeling-guided dose management of oral anticoagulants when initiating nirmatrelvir/ritonavir (Paxlovid) for COVID-19 treatment. *Clin Pharmacol Ther* 2022;**112**:803−7.
37. Honkakoski P, Sueyoshi T, Negishi M. Drug-activated nuclear receptors CAR and PXR. *Ann Med* 2003;**35**:172−82.
38. Ratajewski M, Walczak-Drzewiecka A, Salkowska A, Dastych J. Aflatoxins upregulate *CYP3A4* mRNA expression in a process that involves the PXR transcription factor. *Toxicol Lett* 2011;**205**:146−53.
39. Cheng AS, Zhu J, Lu J, Paine MF, Xie W, Ma X. Chemical basis of pregnane X receptor activators in the herbal supplement Gancao (licorice). *Liver Res* 2022;**6**:251−7.
40. Messina BA. Herbal supplements: facts and myths—talking to your patients about herbal supplements. *J Perianesth Nurs* 2006;**21**: 268−78. quiz 79-81.
41. Lyu M, Fan G, Xiao G, Wang T, Xu D, Gao J, et al. Traditional Chinese medicine in COVID-19. *Acta Pharm Sin B* 2021;**11**: 3337−63.
42. van de Sand L, Bormann M, Alt M, Schipper L, Heilingloh CS, Steinmann E, et al. Glycyrrhizin effectively inhibits SARS-CoV-2 replication by inhibiting the viral main protease. *Viruses* 2021;**13**:609.
43. Buder F, Selejan SR, Hohl M, Kindermann M, Herr C, Lepper PM, et al. Glycyrrhizin through liquorice intake modulates ACE2 and HMGB1 levels—a pilot study in healthy individuals with implications for COVID-19 and ARDS. *PLoS One* 2022;**17**:e0275181.
44. Yepes-Perez AF, Herrera-Calderon O, Oliveros CA, Florez-Alvarez L, Zapata-Cardona MI, Yepes L, et al. The hydroalcoholic extract of *Uncaria tomentosa* (Cat's Claw) inhibits the infection of severe acute respiratory syndrome coronavirus 2 (SARS-CoV-2) *in vitro*. *Evid Based Complement Alternat Med* 2021;**2021**:6679761.
45. Yepes-Perez AF, Herrera-Calderon O, Sanchez-Aparicio JE, Tiessler-Sala L, Marechal JD, Cardona GW. Investigating potential inhibitory effect of *Uncaria tomentosa* (Cat's Claw) against the main protease 3CL(pro) of SARS-CoV-2 by molecular modeling. *Evid Based Complement Alternat Med* 2020;**2020**:4932572.
46. Fahmi OA, Raucy JL, Ponce E, Hassanali S, Lasker JM. Utility of DPX2 cells for predicting CYP3A induction-mediated drug−drug interactions and associated structure−activity relationships. *Drug Metab Dispos* 2012;**40**:2204−11.
47. Tebbens JD, Azar M, Friedmann E, Lanzendorfer M, Pavek P. Mathematical models in the description of pregnane X receptor (PXR)-regulated cytochrome P450 enzyme induction. *Int J Mol Sci* 2018;**19**:1785.
48. Sinz M, Kim S, Zhu Z, Chen T, Anthony M, Dickinson K, et al. Evaluation of 170 xenobiotics as transactivators of human pregnane X receptor (hPXR) and correlation to known CYP3A4 drug interactions. *Curr Drug Metabol* 2006;**7**:375−88.
49. Nijland HM, L'Homme RF, Rongen GA, van Uden P, van Crevel R, Boeree MJ, et al. High incidence of adverse events in healthy volunteers receiving rifampicin and adjusted doses of lopinavir/ritonavir tablets. *AIDS* 2008;**22**:931−5.
50. Haas DW, Koletar SL, Laughlin L, Kendall MA, Suckow C, Gerber JG, et al. Hepatotoxicity and gastrointestinal intolerance when healthy volunteers taking rifampin add twice-daily atazanavir and ritonavir. *J Acquir Immune Defic Syndr* 2009;**50**:290−3.
51. Schmitt C, Riek M, Winters K, Schutz M, Grange S. Unexpected hepatotoxicity of rifampin and saquinavir/ritonavir in healthy male volunteers. *ADI* 2009;**2**:8−16.
52. Jamois C, Riek M, Schmitt C. Potential hepatotoxicity of efavirenz and saquinavir/ritonavir coadministration in healthy volunteers. *ADI* 2009;**2**:1−7.
53. Healan-Greenberg C, Waring JF, Kempf DJ, Blomme EA, Tirona RG, Kim RB. A human immunodeficiency virus protease inhibitor is a novel functional inhibitor of human pregnane X receptor. *Drug Metab Dispos* 2008;**36**:500−7.
54. Sharma D, Lau AJ, Sherman MA, Chang TK. Agonism of human pregnane X receptor by rilpivirine and etravirine: comparison with first generation non-nucleoside reverse transcriptase inhibitors. *Biochem Pharmacol* 2013;**85**:1700−11.
55. Bertilsson G, Heidrich J, Svensson K, Asman M, Jendeberg L, Sydow-Backman M, et al. Identification of a human nuclear receptor defines a new signaling pathway for CYP3A induction. *Proc Natl Acad Sci U S A* 1998;**95**:12208−13.